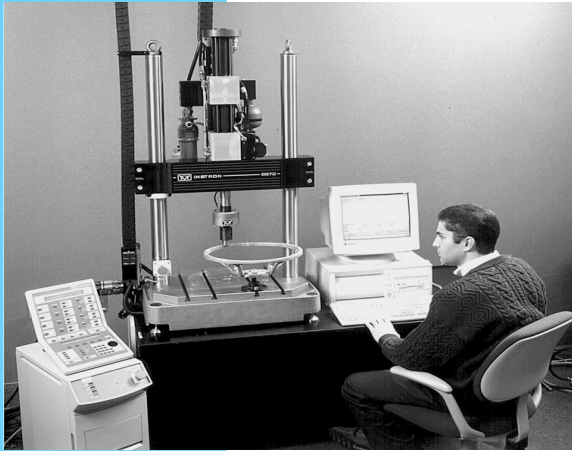
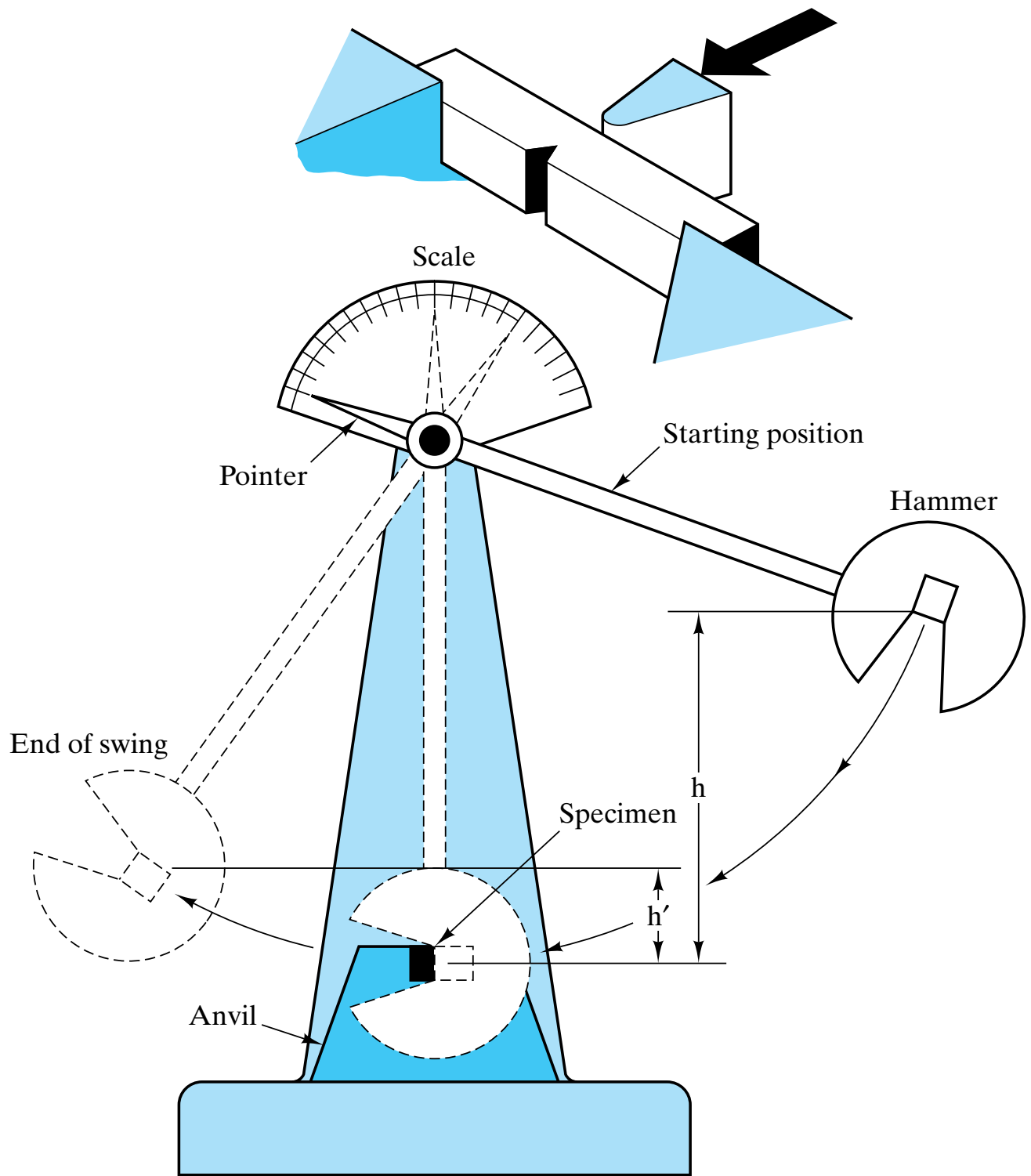


# CHAPTER 8

## Failure Analysis and Prevention



*The repetitive loading of engineering materials opens up additional opportunities for structural failure. Shown here is a mechanical testing machine, introduced in Chapter 6, modified to provide rapid cycling of a given level of mechanical stress. The resulting fatigue failure is a major concern for design engineers. (Courtesy of Instron Corporation)*



**Figure 8-1** Charpy test of impact energy. (From H. W. Hayden, W. G. Moffatt, and J. Wulff, *The Structure and Properties of Materials, Vol. 3: Mechanical Behavior*, John Wiley & Sons, Inc., New York, 1965.)

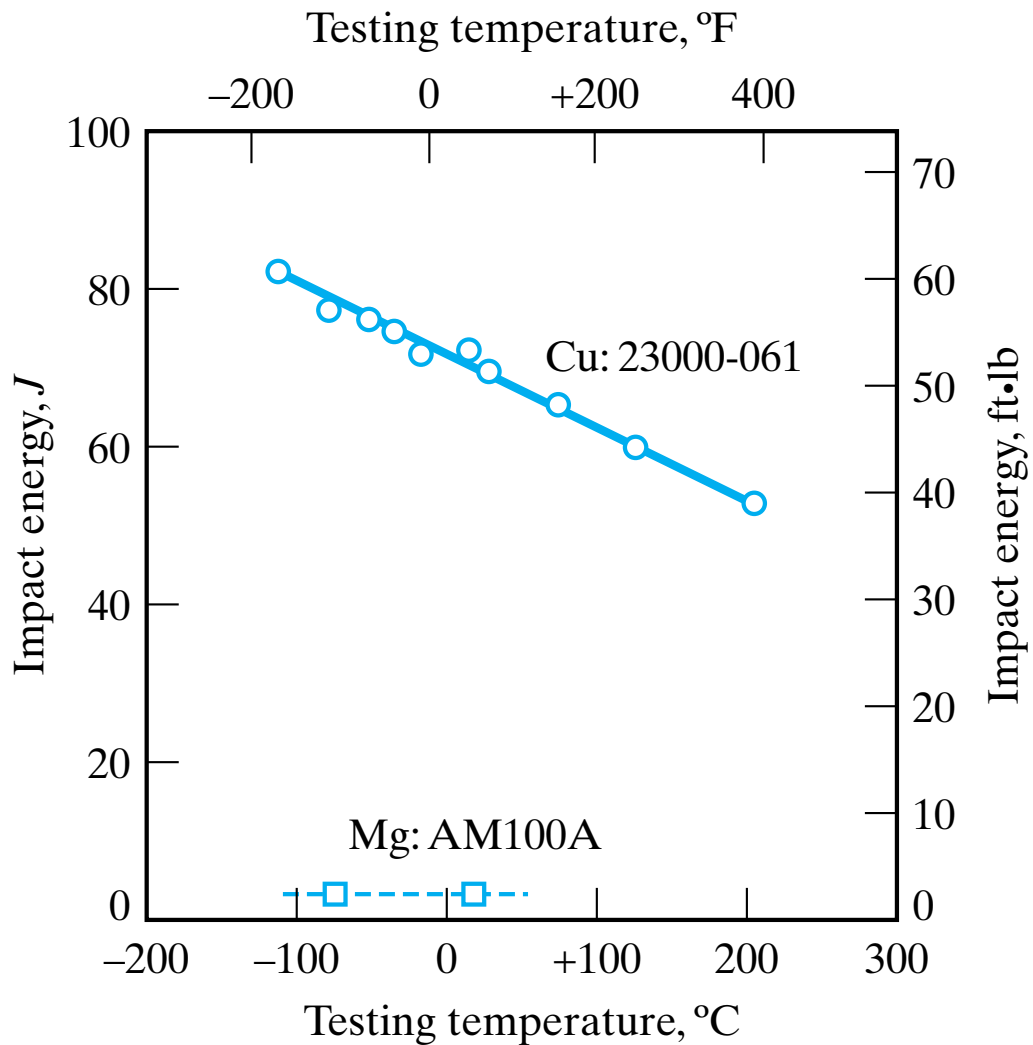


**Figure 8-2** *Impact energy for a ductile fcc alloy (copper C23000–061, “red brass”) is generally high over a wide temperature range. Conversely, the impact energy for a brittle hcp alloy (magnesium AM100A) is generally low over the same range. (From Metals Handbook, 9th Ed., Vol. 2, American Society for Metals, Metals Park, Ohio, 1979.)*

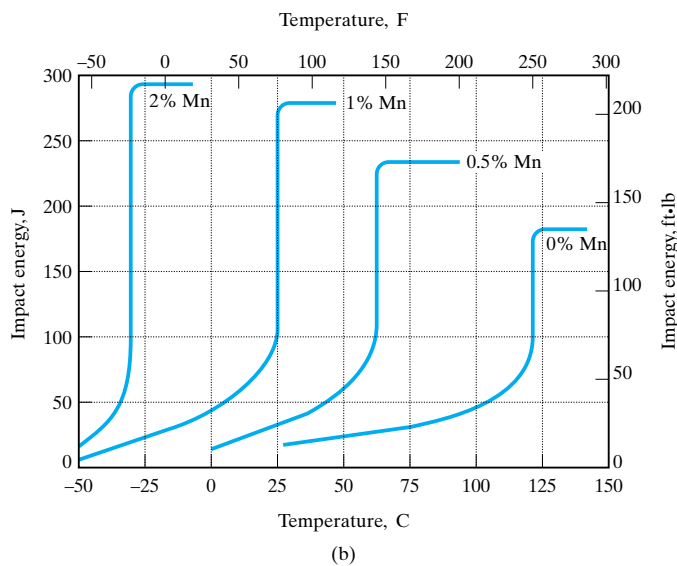
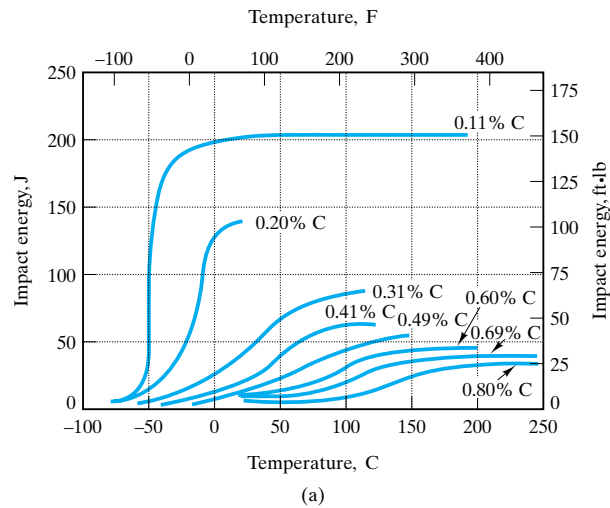
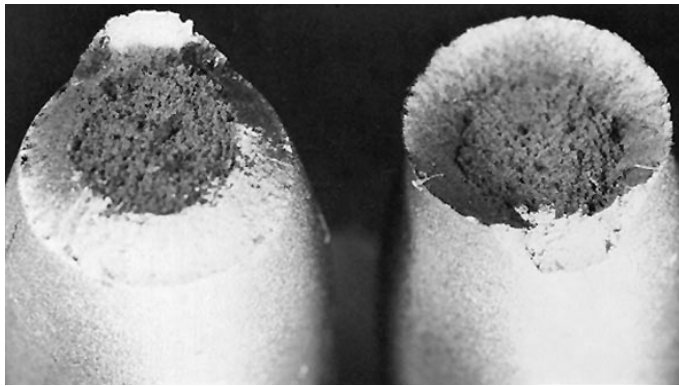
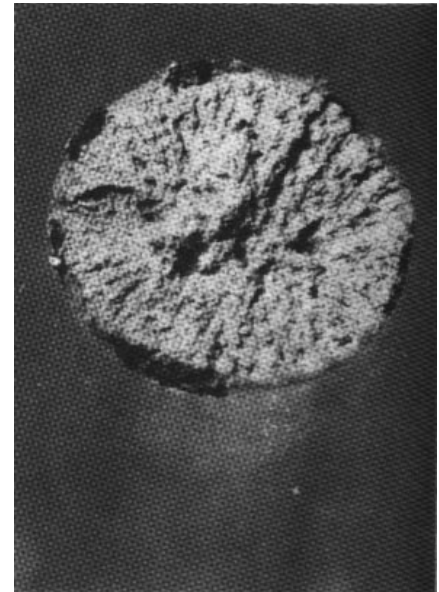


**Figure 8-3** Variation in ductile-to-brittle transition temperature with alloy composition. (a) Charpy V-notch impact energy with temperature for plain-carbon steels with various carbon levels (in weight percent). (b) Charpy V-notch impact energy with temperature for Fe–Mn–0.05C alloys with various manganese levels (in weight percent). (From Metals Handbook, 9th Ed., Vol. 1, American Society for Metals, Metals Park, Ohio, 1978.)

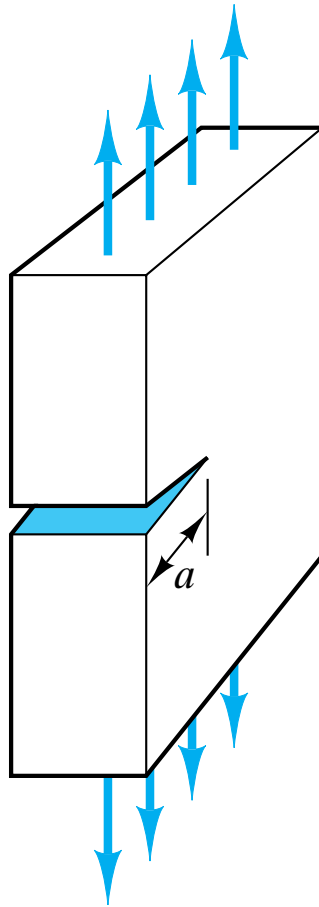


(a)

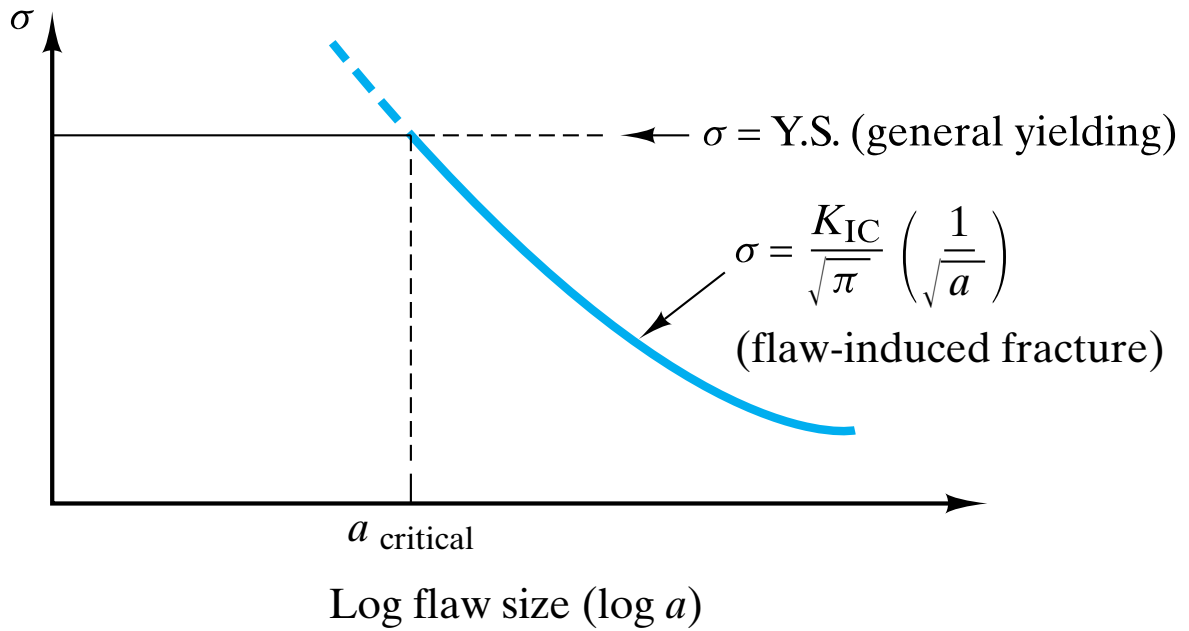


(b)

**Figure 8-4** (a) Typical “cup and cone” ductile fracture surface. Fracture originates near the center and spreads outward with a dimpled texture. Near the surface, the stress state changes from tension to shear with fracture continuing at approximately  $45^\circ$ . (From Metals Handbook, 9th Ed., Vol. 12, ASM International, Metals Park, Ohio, 1987.) (b) Typical cleavage texture of brittle fracture surface. (From Metals Handbook, 9th Ed., Vol. 11, American Society Metals, Metals Park, Ohio, 1986.)

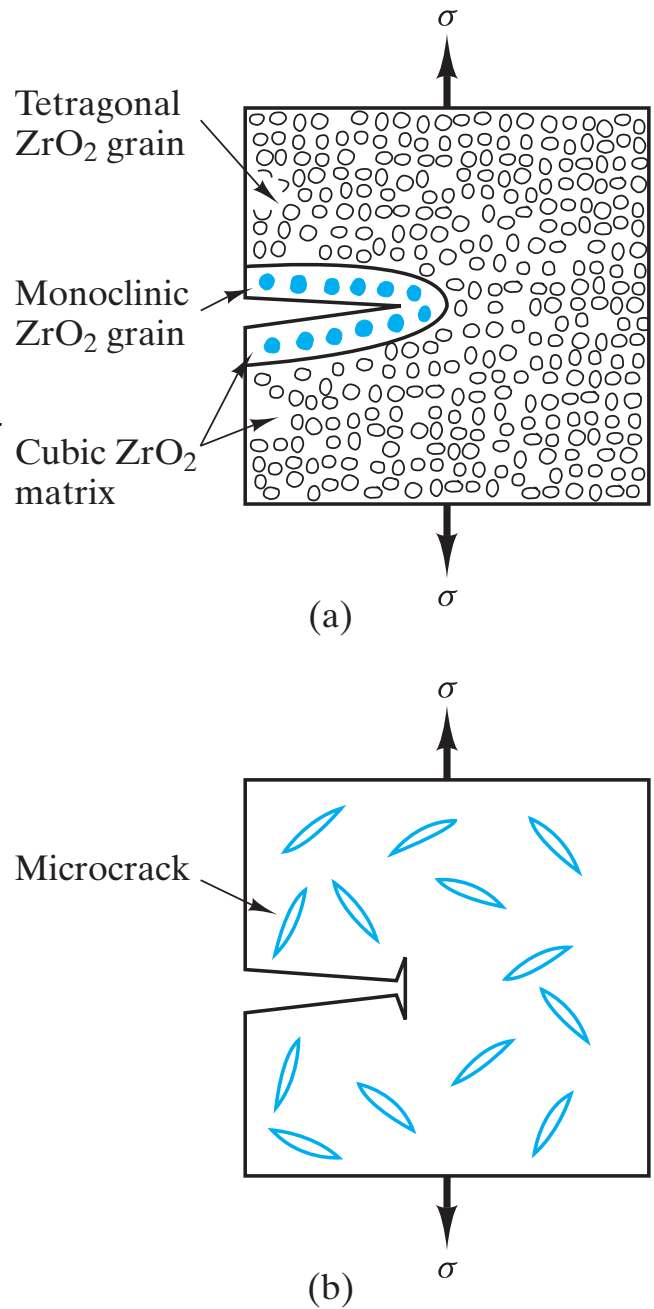


**Figure 8-5** *Fracture toughness test.*



**Figure 8-6** A design plot of stress versus flaw size for a pressure vessel material in which general yielding occurs for flaw sizes less than a critical size,  $a_{\text{critical}}$ , but catastrophic “fast fracture” occurs for flaws larger than  $a_{\text{critical}}$ .

**Figure 8-7** Two mechanisms for improving fracture toughness of ceramics by crack arrest. (a) Transformation toughening of partially stabilized zirconia involves the stress-induced transformation of tetragonal grains to the monoclinic structure which has a larger specific volume. The result is a local volume expansion at the crack tip, squeezing the crack shut and producing a residual compressive stress. (b) Microcracks produced during fabrication of the ceramic can blunt the advancing crack tip.





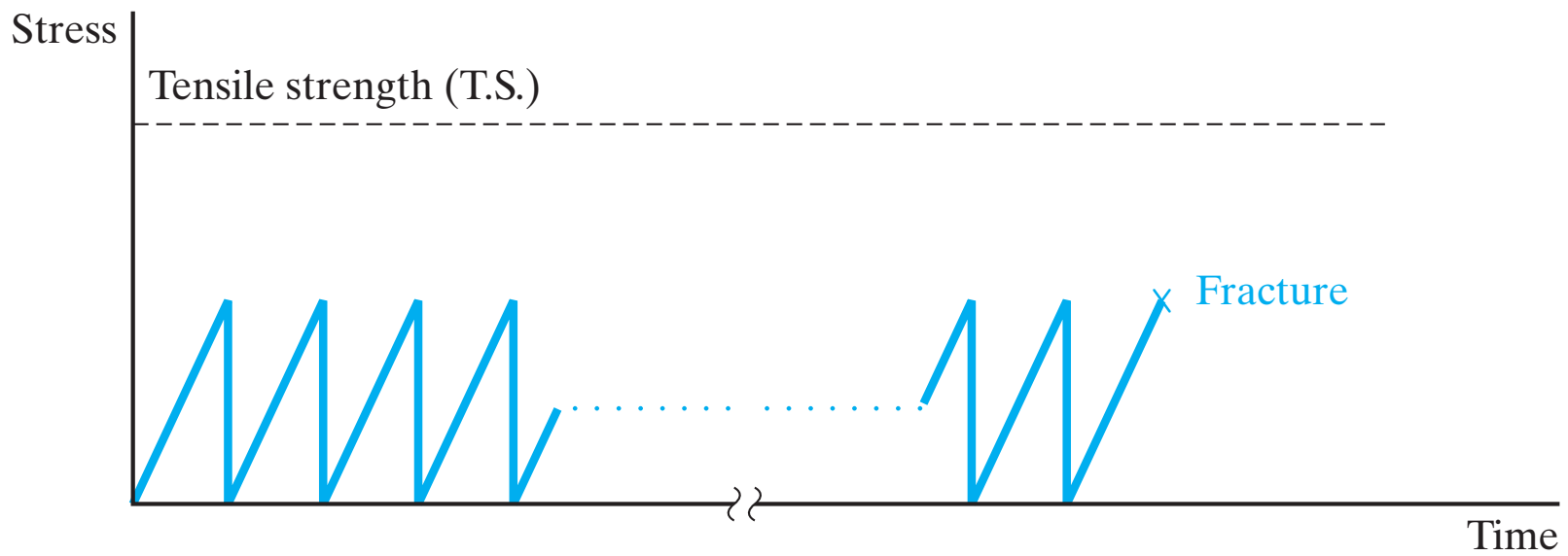


**Figure 8-8** *Fatigue corresponds to the brittle fracture of an alloy after a total of  $N$  cycles to a stress below the tensile strength.*

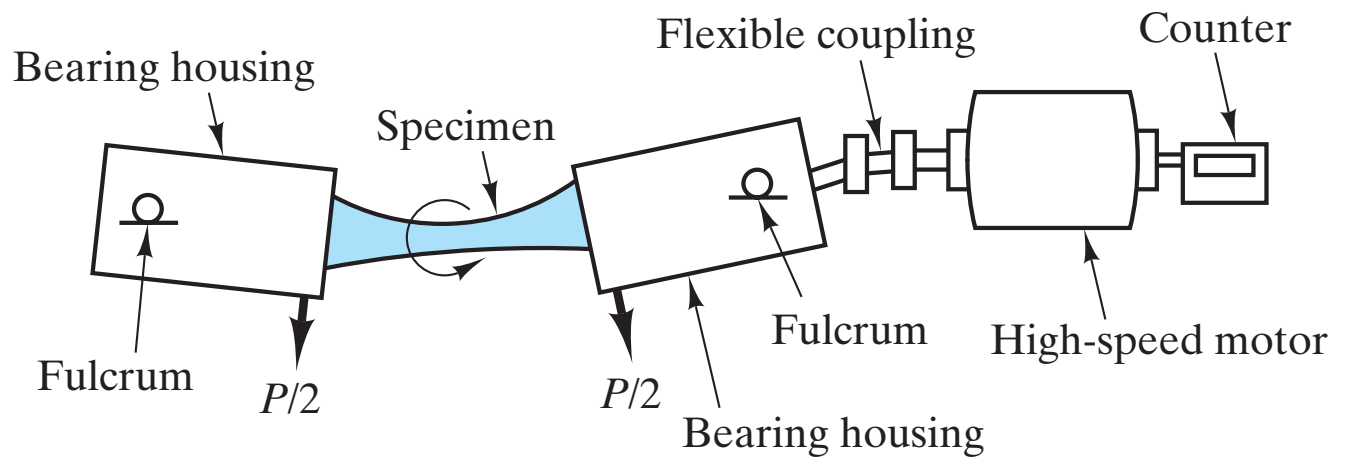


**Figure 8-9** *Fatigue test.* (From C. A. Keyser, *Materials Science in Engineering*, 4th Ed., Charles E. Merrill Publishing Company, Columbus, Ohio, 1986.)

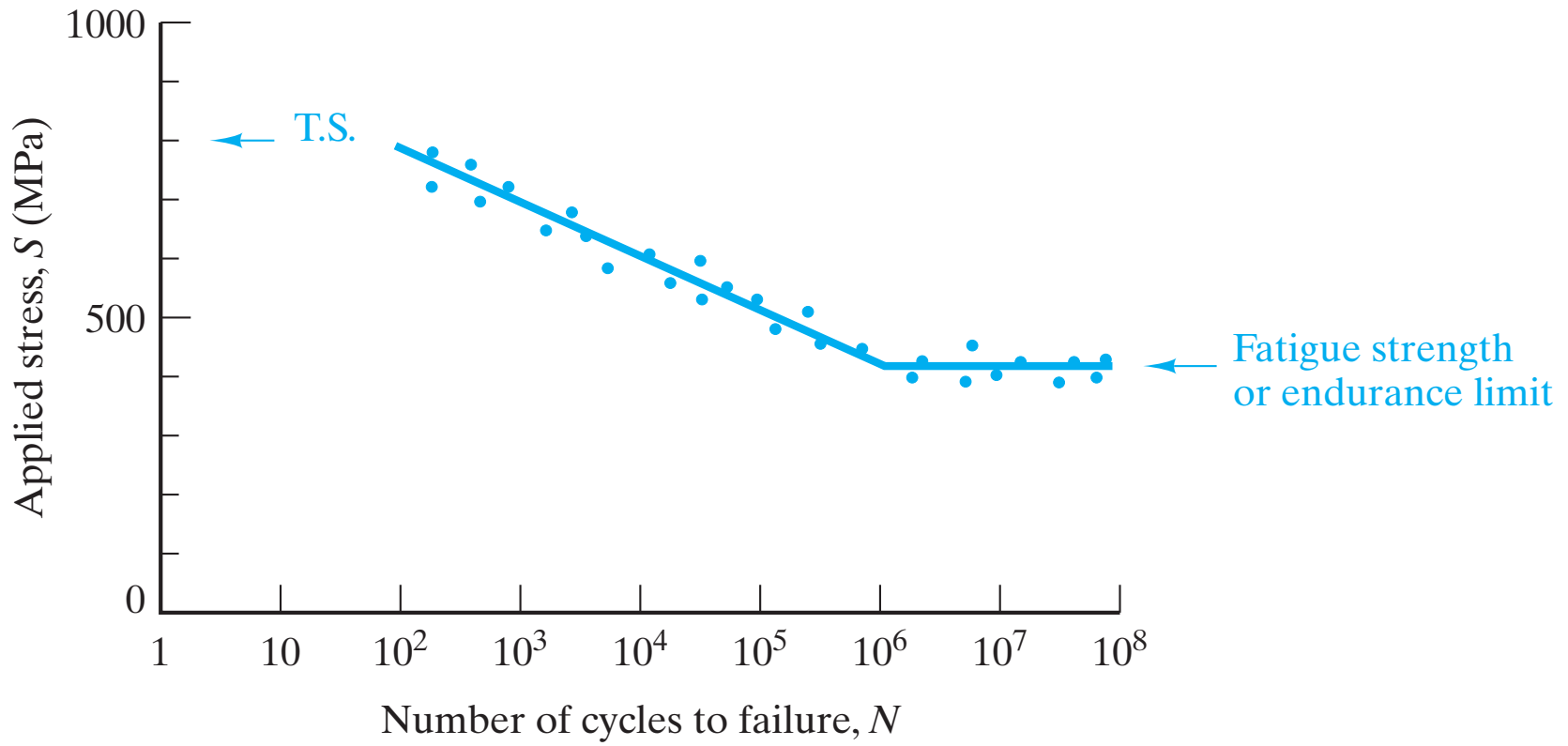


**Figure 8-10** Typical fatigue curve. (Note that a log scale is required for the horizontal axis.)

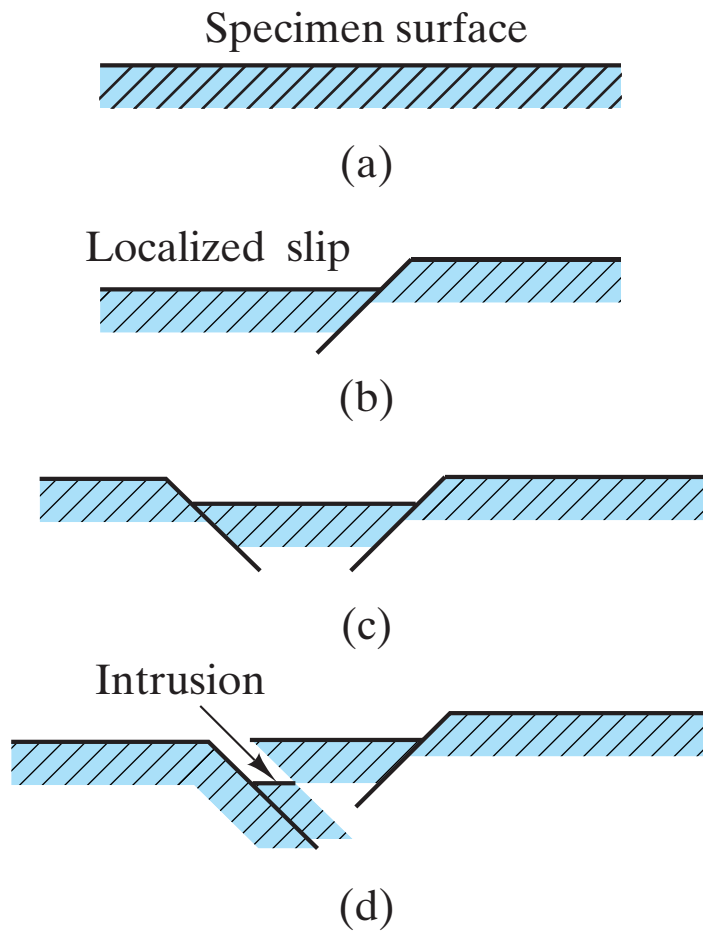


**Figure 8-11** *An illustration of how repeated stress applications can generate localized plastic deformation at the alloy surface leading eventually to sharp discontinuities.*

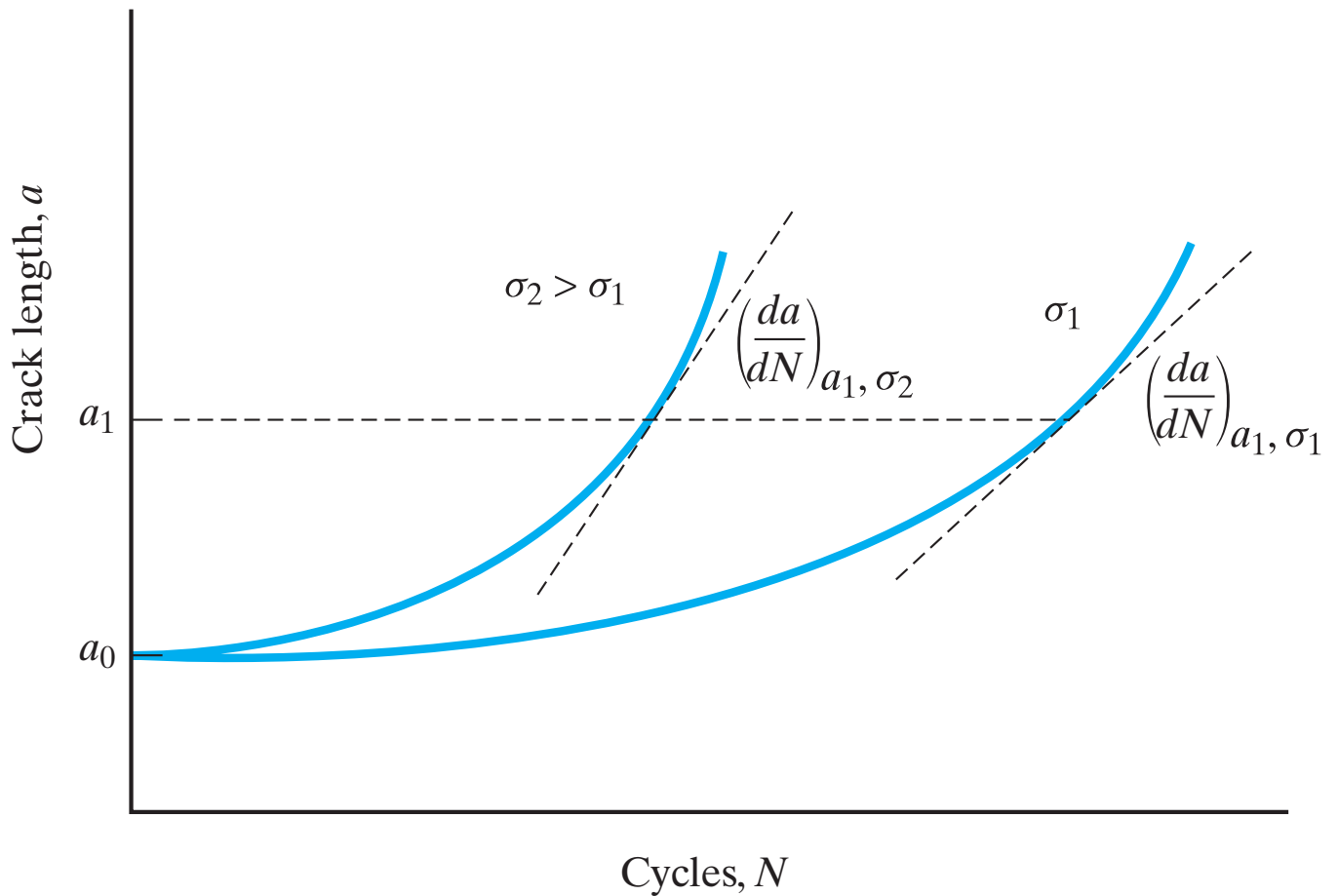


**Figure 8-12** Illustration of crack growth with number of stress cycles,  $N$ , at two different stress levels. Note that, at a given stress level, the crack growth rate,  $da/dN$ , increases with increasing crack length, and, for a given crack length such as  $a_1$ , the rate of crack growth is significantly increased with increasing magnitude of stress.

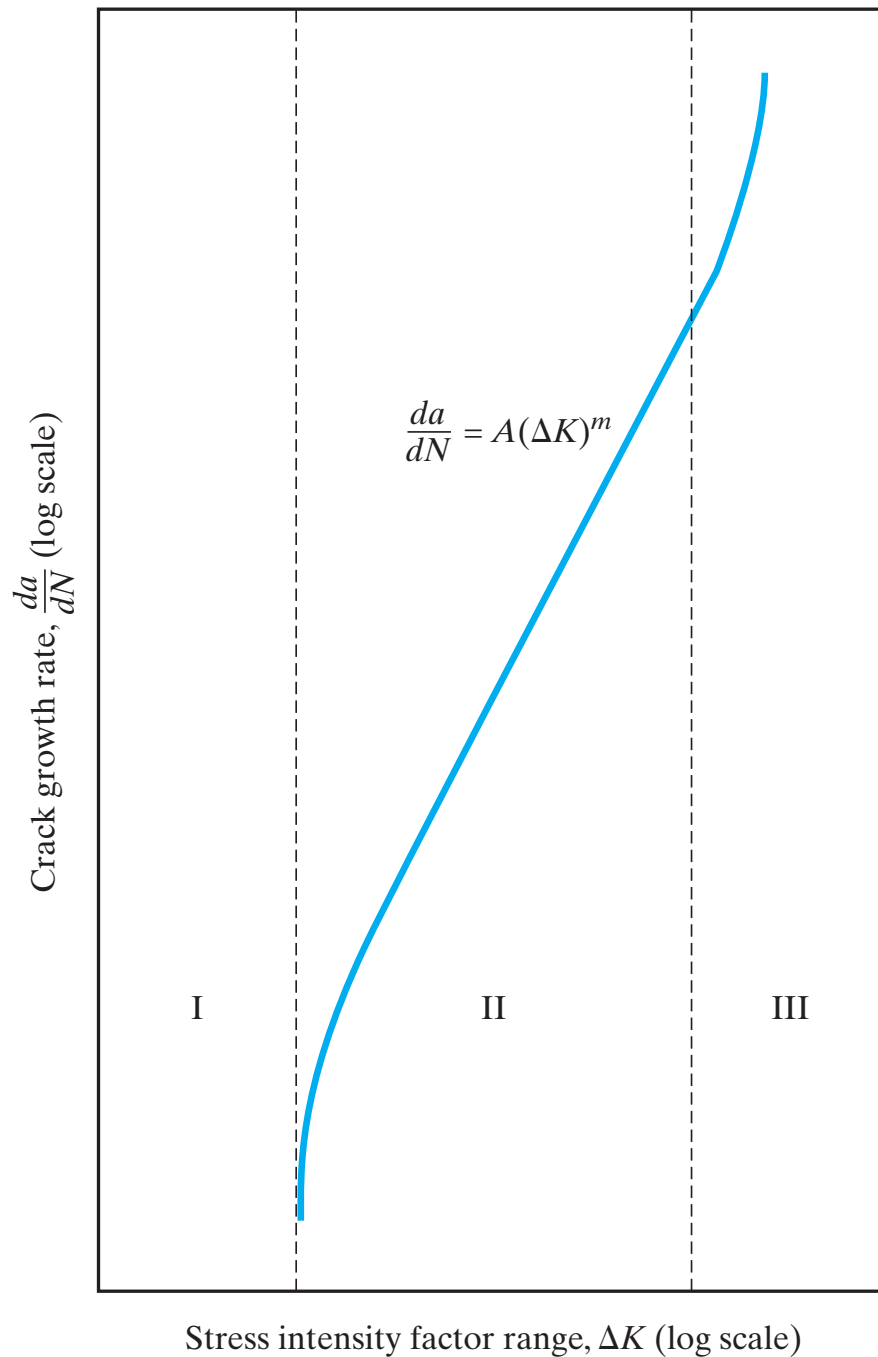


**Figure 8-13** Illustration of logarithmic relationship between crack growth rate,  $da/dN$ , and the stress intensity factor range,  $\Delta K$ . Region I corresponds to nonpropagating fatigue cracks. Region II corresponds to a linear relationship between  $\log da/dN$  and  $\log \Delta K$ . Region III represents unstable crack growth prior to catastrophic failure.

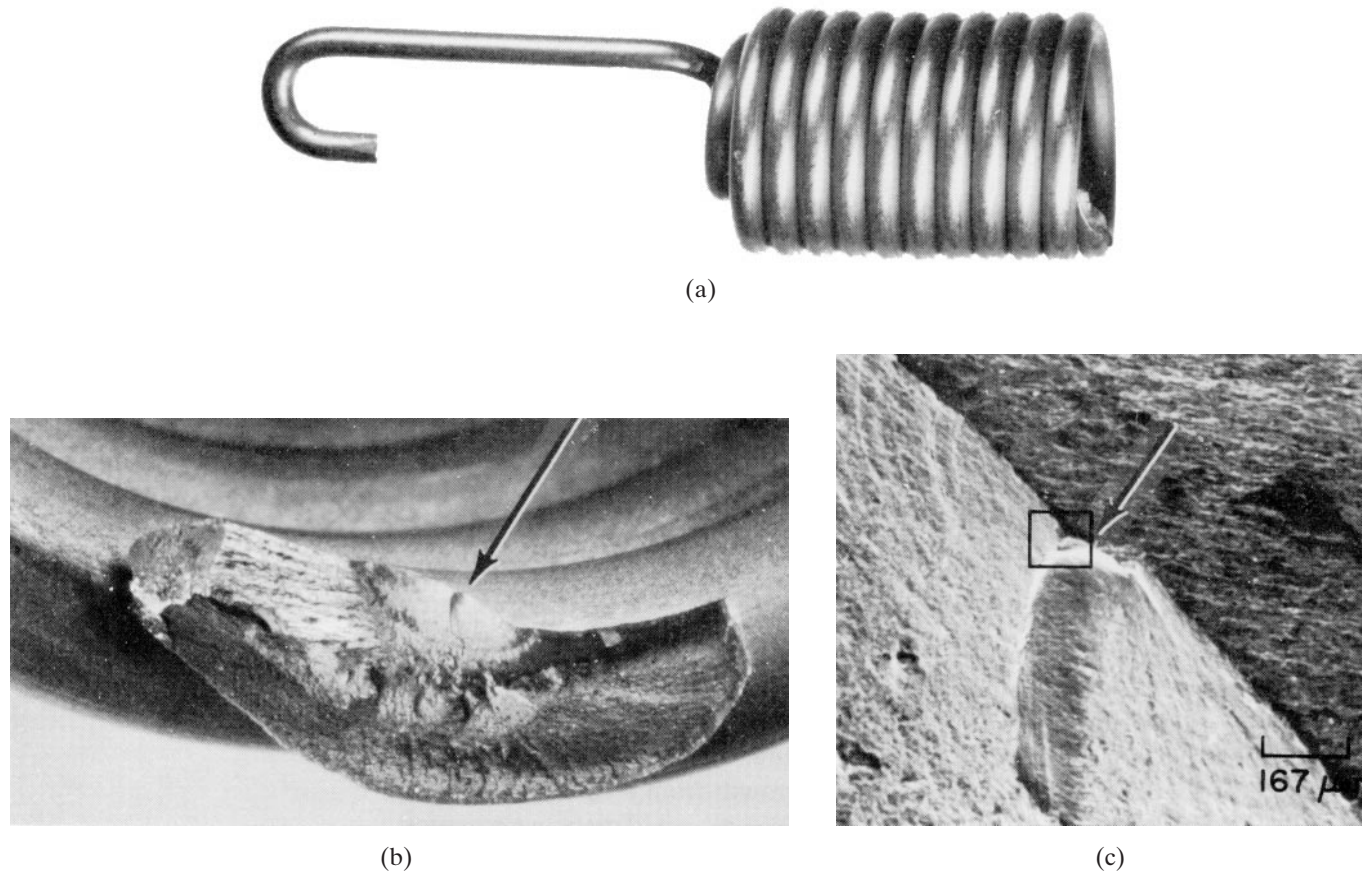
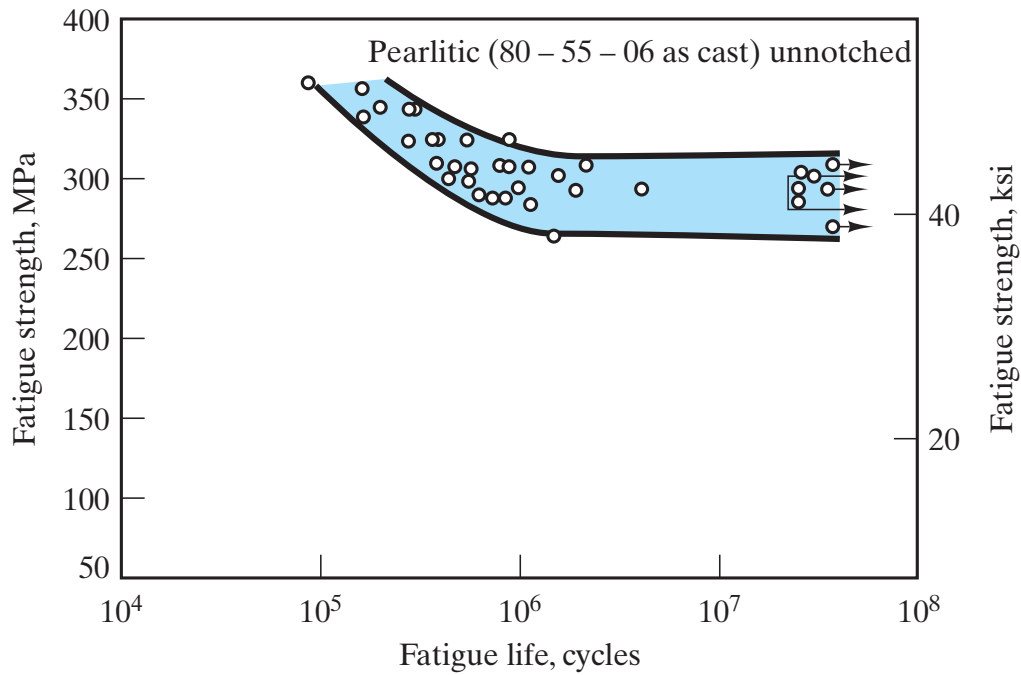
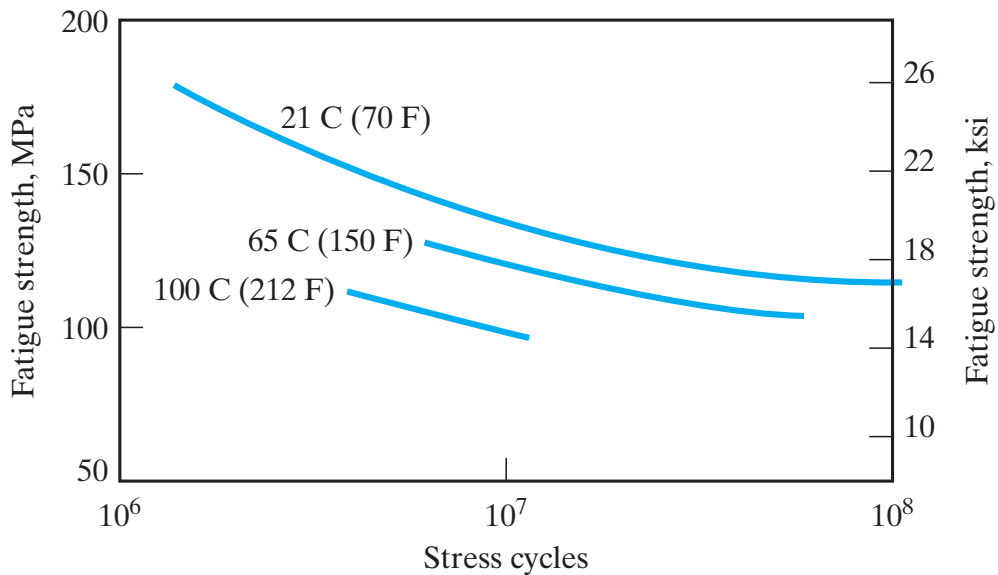


**Figure 8-14** Characteristic fatigue fracture surface. (a) Photograph of an aircraft throttle-control spring ( $1\frac{1}{2}\times$ ) that broke in fatigue after 274 h of service. The alloy is 17-7PH stainless steel. (b) Optical micrograph ( $10\times$ ) of the fracture origin (arrow) and the adjacent smooth region containing a concentric line pattern as a record of cyclic crack growth (an extension of the surface discontinuity shown in Figure 8-11). The granular region identifies the rapid crack propagation at the time of failure. (c) Scanning electron micrograph ( $60\times$ ), showing a closeup of the fracture origin (arrow) and adjacent “clamshell” pattern. (From Metals Handbook, 8th Ed., Vol. 9: Fractography and Atlas of Fractographs, American Society for Metals, Metals Park, Ohio, 1974.)



(a)



(b)

**Figure 8-15** Comparison of fatigue curves for (a) ferrous and (b) nonferrous alloys. The ferrous alloy is a ductile iron. The nonferrous alloy is C11000 copper wire. The nonferrous data do not show a distinct endurance limit, but the failure stress at  $N = 10^8$  cycles is a comparable parameter. (After Metals Handbook, 9th Ed., Vols. 1 and 2, American Society for Metals, Metals Park, Ohio, 1978, 1979.)



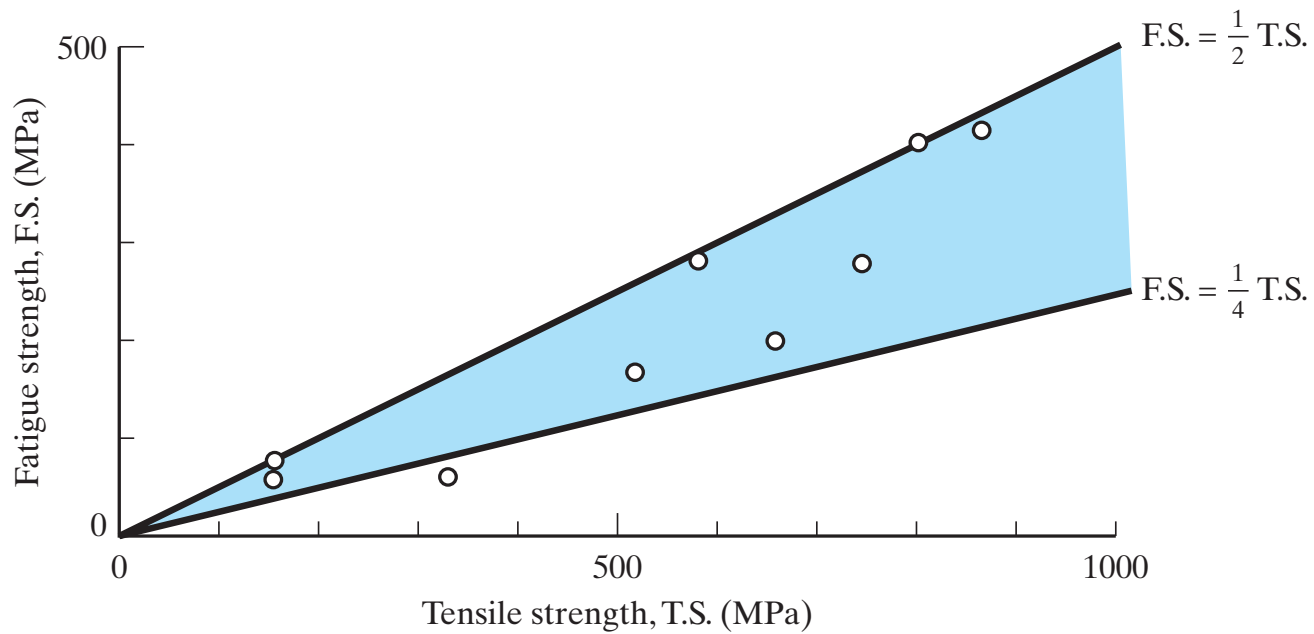


**Figure 8-16** Plot of data from Table 8.4 showing how fatigue strength is generally one-fourth to one-half of the tensile strength.

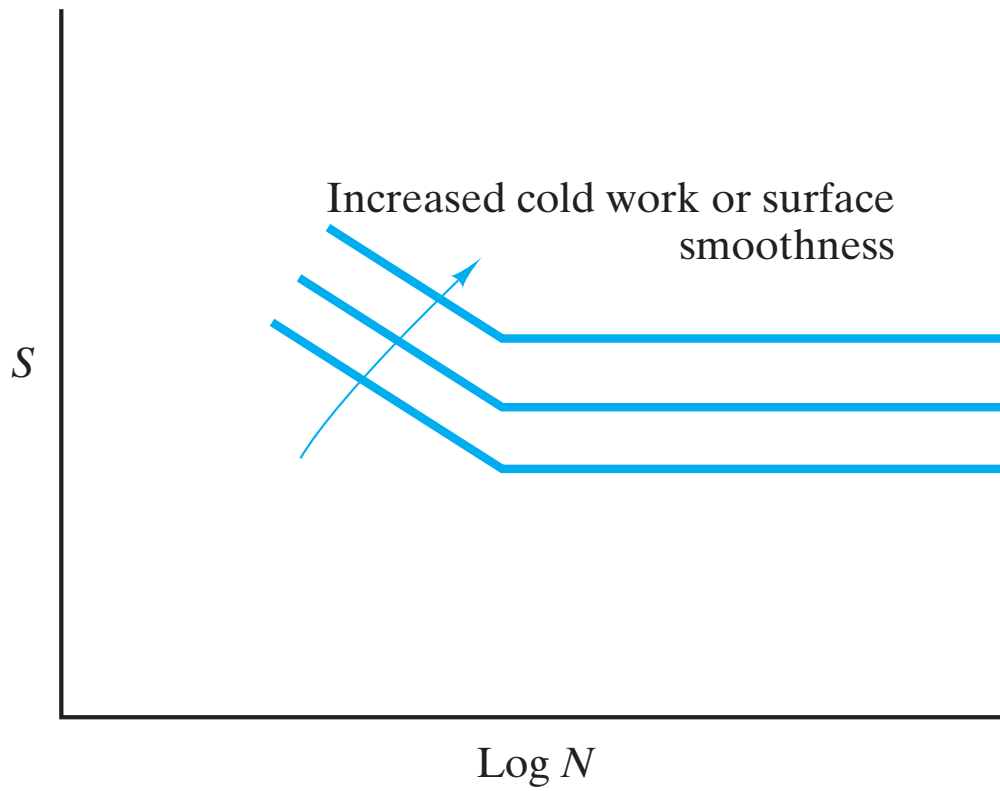


**Figure 8-17** *Fatigue strength is increased by prior mechanical deformation or reduction of structural discontinuities.*

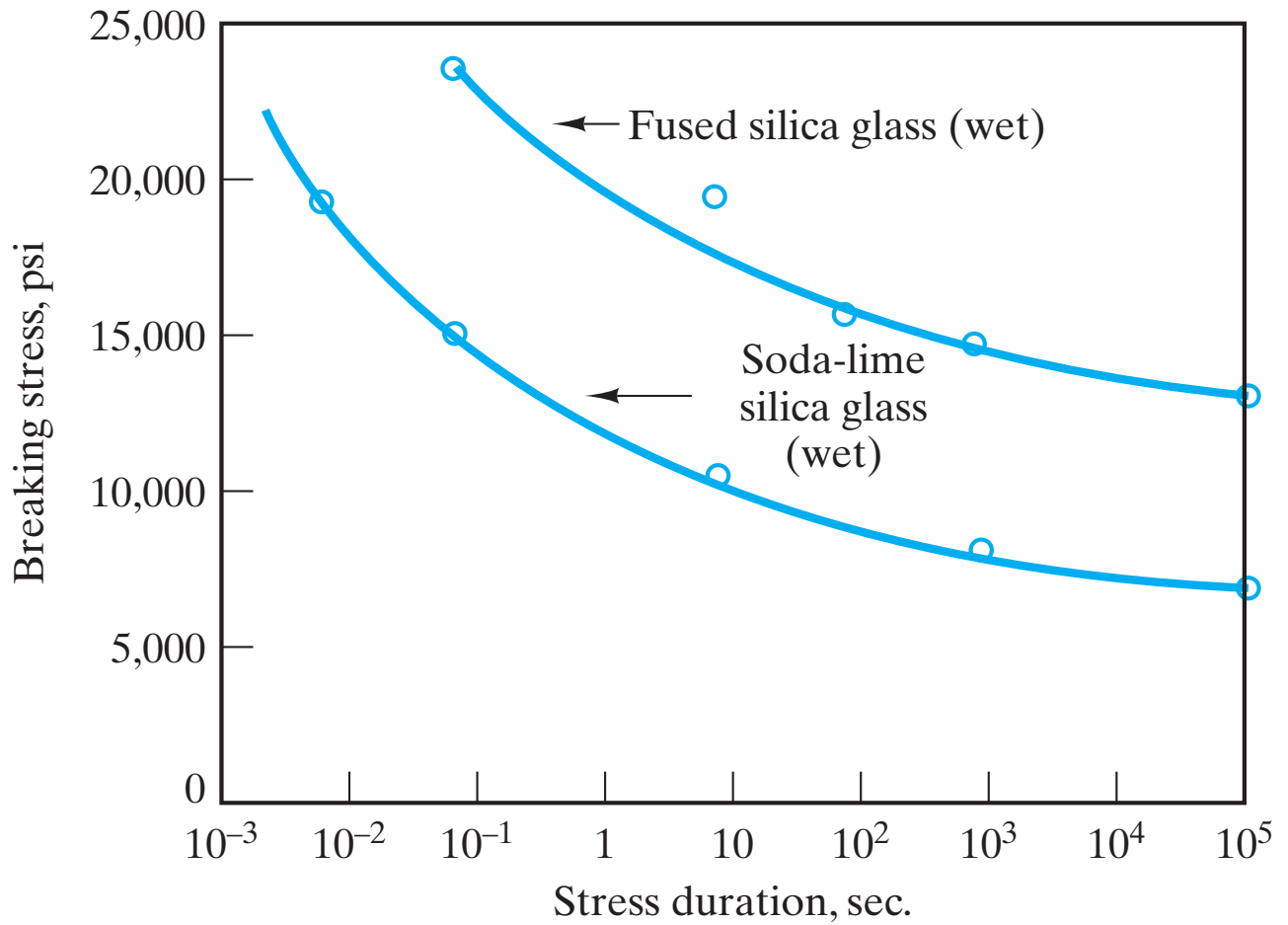


**Figure 8-18** *The drop in strength of glasses with duration of load (and without cyclic load applications) is termed static fatigue. (From W. D. Kingery, Introduction to Ceramics, John Wiley & Sons, Inc., New York, 1960.)*

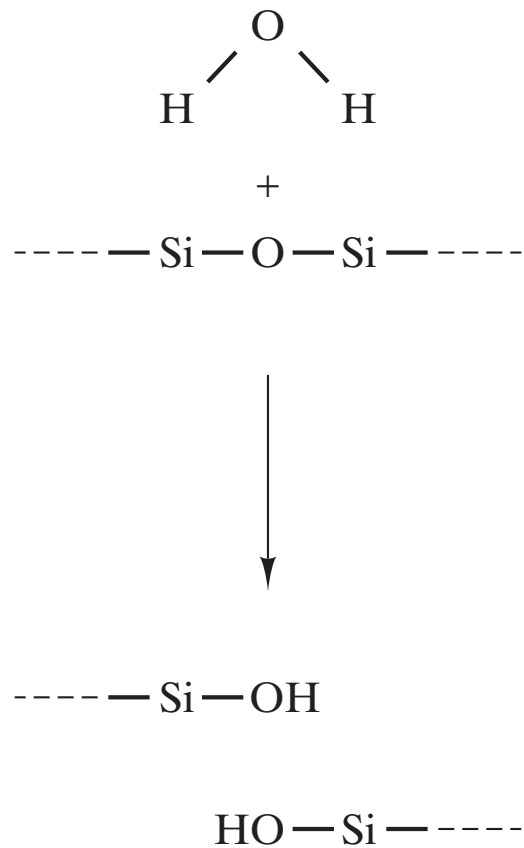
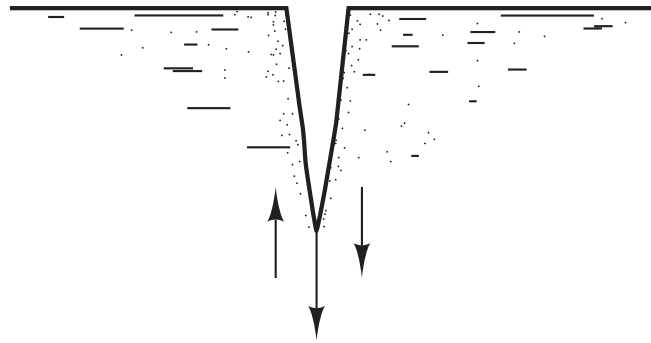
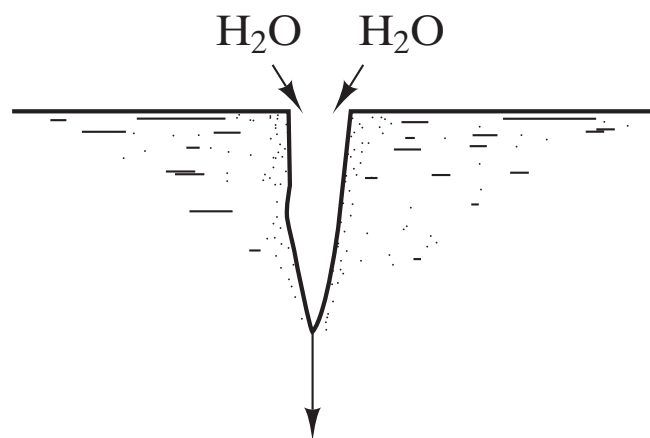


**Figure 8-19** *The role of H<sub>2</sub>O in static fatigue depends on its reaction with the silicate network. One H<sub>2</sub>O molecule and one -Si-O-Si- segment generate two Si-OH units. This is equivalent to a break in the network.*



Crack growth by local shearing mechanism

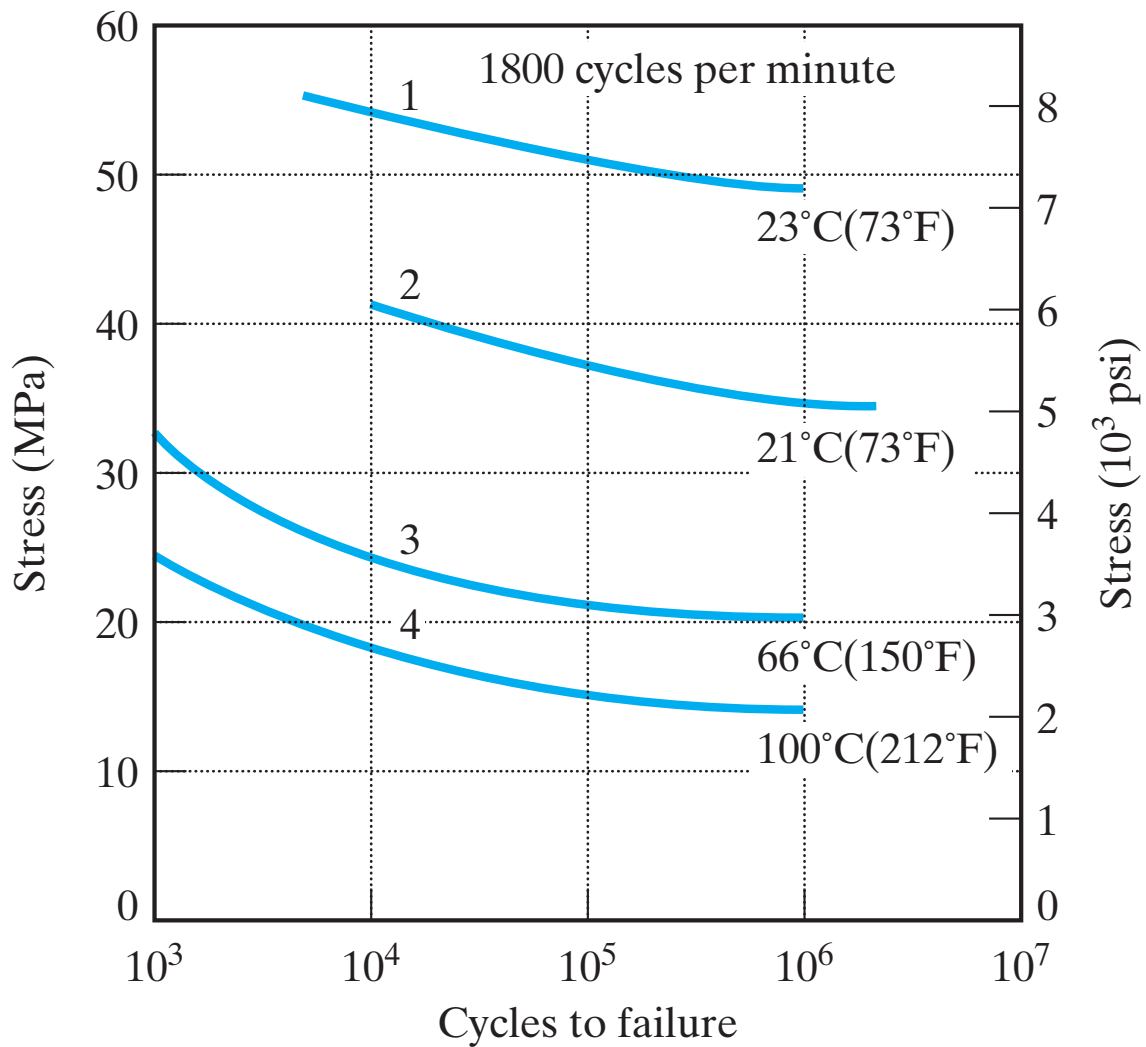
(a)



Crack growth by chemical breaking of  
oxide network

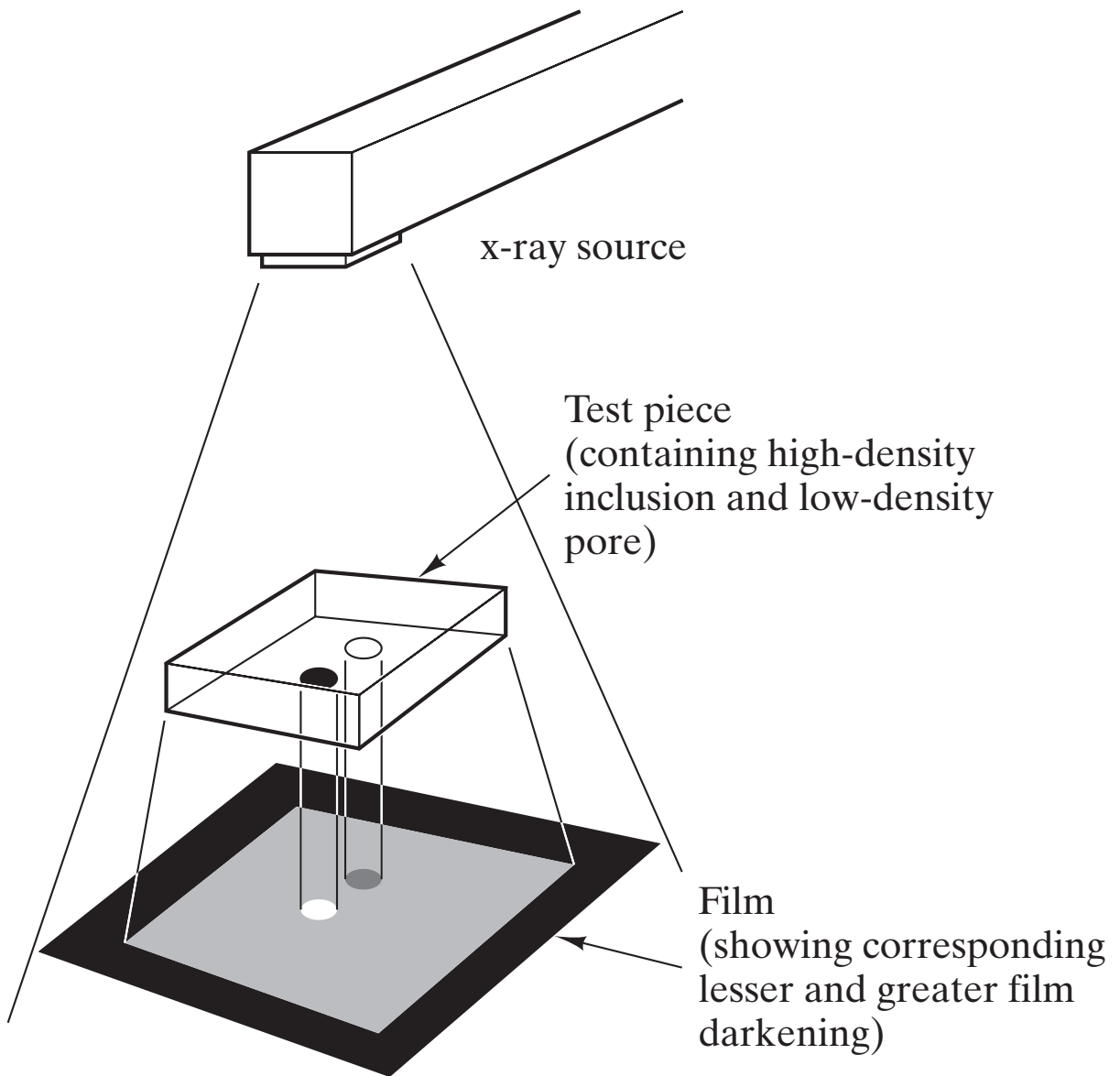
(b)

**Figure 8-20** Comparison of (a) cyclic fatigue in metals and (b) static fatigue in ceramics.

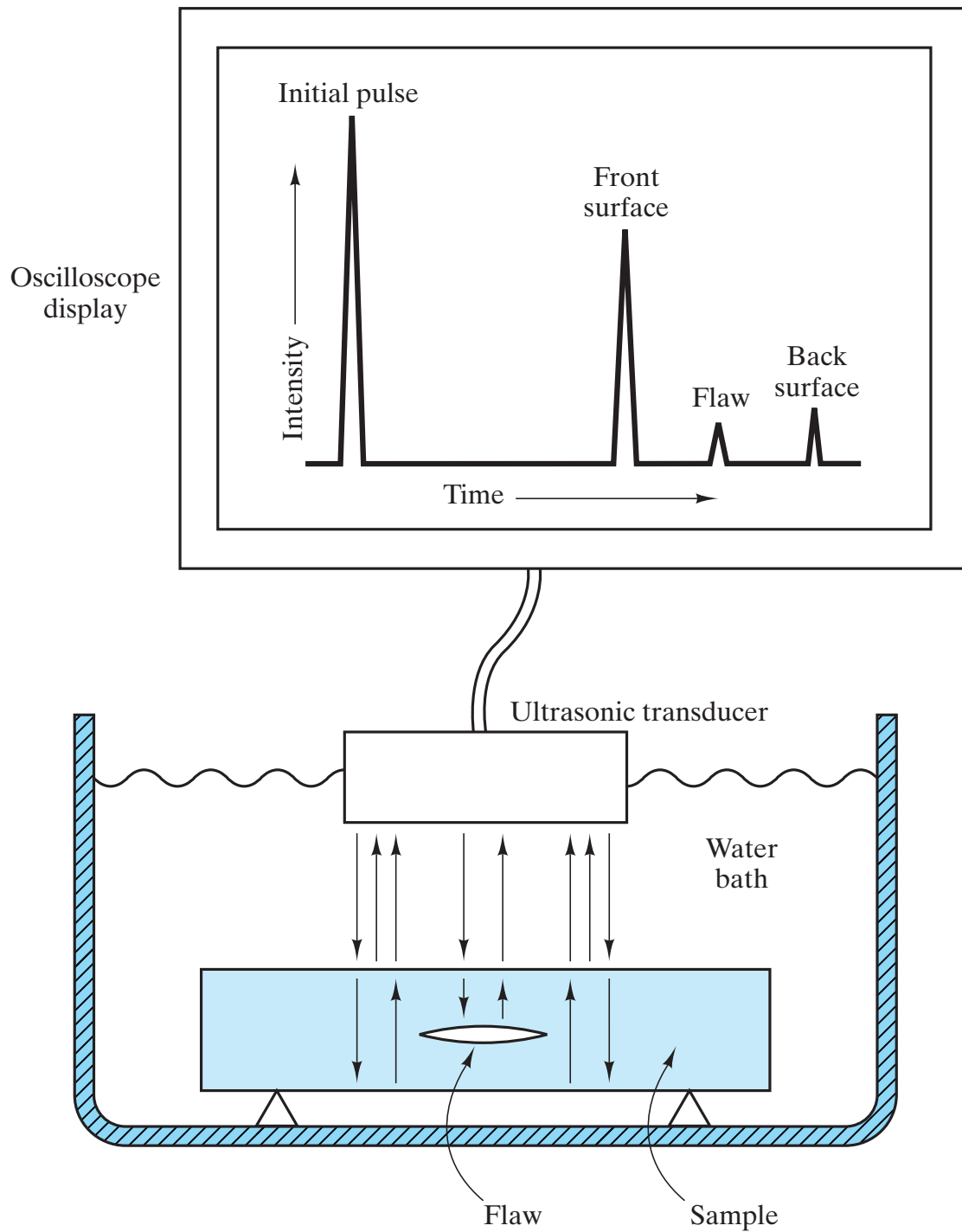


1. Tensile stress only
2. Completely reversed tensile and compressive stress
3. Completely reversed tensile and compressive stress
4. Completely reversed tensile and compressive stress

**Figure 8-21** Fatigue behavior for an acetal polymer at various temperatures. (From Design Handbook for Du Pont Engineering Plastics, used by permission.)

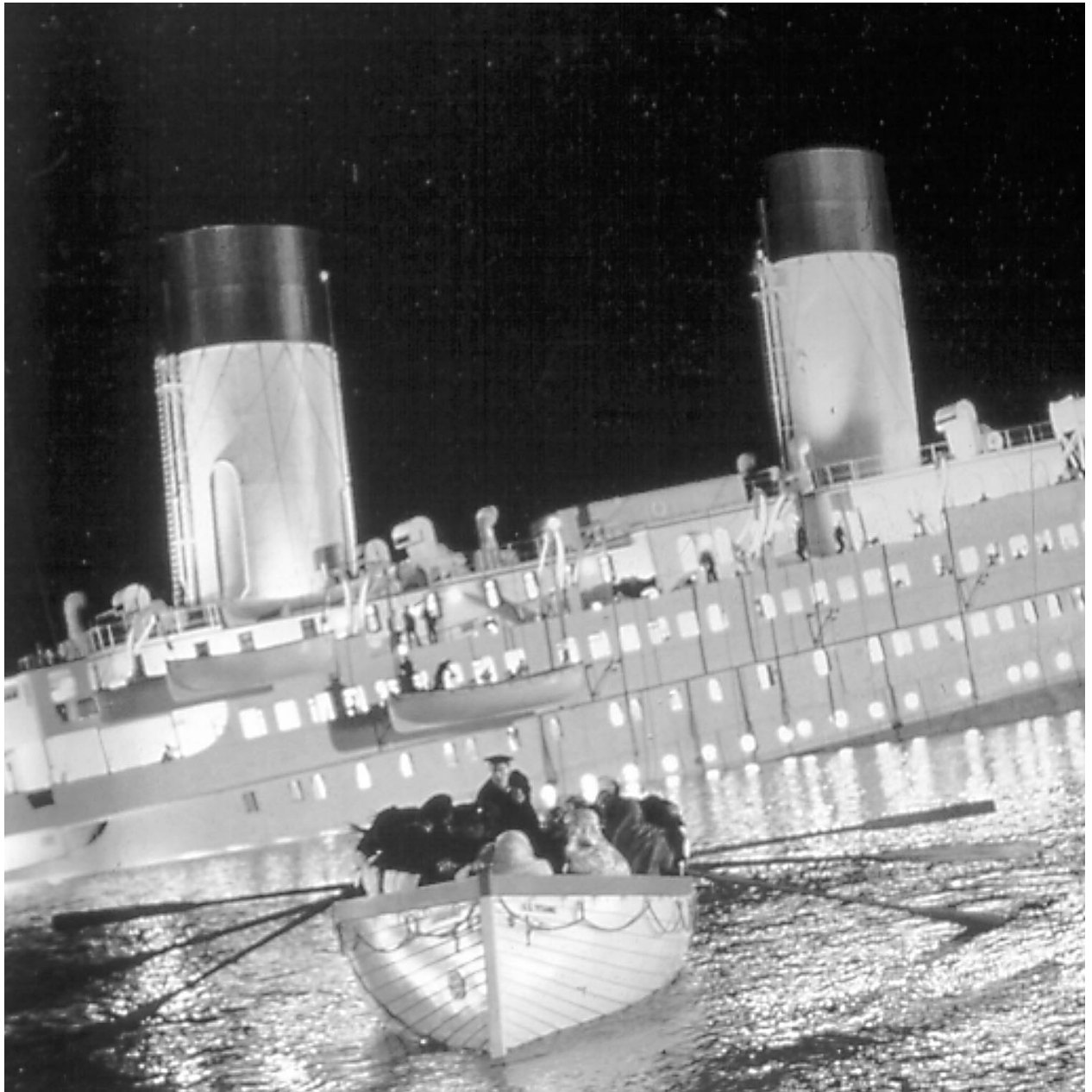


**Figure 8-22** *A schematic of x-radiography.*



**Figure 8-23** *A schematic of a “pulse echo” ultrasonic test.*





*(Courtesy of Paramount Pictures and Twentieth Century Fox)*